SURFACE ENERGY ANISOTROPY FOR THE LOW-INDEX CRYSTAL SURFACES OF THE TEXTURED POLYCRYSTALLINE BCC TUNGSTEN: EXPERIMENTAL AND THEORETICAL ANALYSIS

A.I. Belyaeva[1], A.A. Savchenko[1], A.A. Galuza[1], I.V. Kolenov[2,3]
[1]National Technical University "Kharkov Polytechnic Institute", Kharkov, Ukraine;
[2]Institute of Electrophysics and Radiation Technologies of NAS of Ukraine, Kharkov, Ukraine;
[3]O.Ya. Usikov Institute for Radiophysics and Electronics of NAS of Ukraine, Kharkov, Ukraine
E-mail: alla.iv.belyaeva@gmail.com, alexey.galuza@gmail.com

Summarizing the experimental and theoretical trends observed on the changes in surface microstructure and topography resulting from surface energy anisotropy for the low-index crystal surfaces of the polycrystalline bcc tungsten under sputtering is done. A brief summary of the most closely related work is included. The experimental results have been discussed in the framework of the various theoretical methods. Emphasis was placed on the problems which are existing up to now. It is shown that the absence of a common trend in the ordering of the (100), (110), and (111) surface energies amongst the various theoretical models is a problem yet to be satisfactorily discussed. It is shown experimentally that for polycrystalline textured tungsten (bcc metal), the order of the three low-index surface energies is $\gamma_{(111)} > \gamma_{(100)} > \gamma_{(110)}$.

PACS: 79.20.Rf, 68.35.Ct, 65.40.gp

INTRODUCTION AND MOTIVATION

Over the past few years, there have been many of manuscripts published reporting different aspects of sputtering. In particular, surface sputtering was used as an instrument for studying the surface energy of the low-index crystal surfaces of the polycrystalline tungsten. The purpose of this article is to summarize the experimental and theoretical trends observed when bcc tungsten is exposed to an energetic ion beam.

Tungsten (W) is a body-centered-cubic (bcc) metal with very high melting point (3695 K) and high density (19.35 g/cm^3) [1]. Due to its unique properties, W and its alloys have been applied in many fields, such as lighting engineering, electronics industry, aerospace and military field, medical and especially nuclear field. In order to meet various applications, different microstructures, thermomechanical properties, and textures are desired to be obtained. For example, recent literature indicated that W grains with certain crystallographic orientation exhibited excellent irradiation resistance under deuterium (D), helium (He) and other ions sputtering. In this context, understanding nature and value of surface energy need to be recognized as an important challenge.

Surface energy is defined as the surface excess free energy per unit area of a particular crystal facet and is one of the basic quantities in surface physics. It determines the equilibrium shape of crystals and plays an important role in faceting, roughening, crystal growth phenomena and more. The lack of direct experimental data leads to a number of different numerical methods for modeling surface energy.

In recent years, there have been many calculations of the surface energy of bcc metals either from first-principles or by semi-empirical methods. A brief summary of the most closely related work is included in [2] (and in references therein). All of these methods are mathematically similar and have in common the attribute that the interaction between two atoms depends upon their local environment. It is mainly this fact that accounts for the huge successes that these methods have had in predicting effects at metallic surfaces where the atomic environment is significantly different from the bulk. The theoretical problem of calculating the surface energies of bcc metals is still to be satisfactorily solved. The differences in the results obtained by the several theoretical methods are not yet small enough for us to begin to think that the different calculations have converged. In particular, up today the absence of a common trend in the ordering of the (100), (110), and (111) bcc metals surface energies amongst the various theoretical models is a problem yet to be satisfactorily discussed. Some authors support the trend $\gamma_{(110)} < \gamma_{(100)} < \gamma_{(111)}$, but the others – the other trend $\gamma_{(110)} < \gamma_{(111)} < \gamma_{(100)}$. Thus, the problem is open now.

The purpose of this article is to summarize the experimental and theoretical trends observed on the changes in surface microstructure and topography resulting from surface energy anisotropy for the low-index crystal surfaces of the polycrystalline bcc tungsten under sputtering. A brief summary of the most closely related work is included here. The experimental results are discussed in the framework of the various theoretical methods. Emphasis is placed on the problems which exist now.

1. EXPERIMENTALLY MEASURED SPUTTERING YIELDS AND SURFACE ENERGY OF BCC TUNGSTEN

Tungsten has been considered to be a potential candidate for the first wall material in a fusion reactor due to its unique physical and electrochemical properties including high thermal conductivity, low evaporation rate, very low sputtering yield, and high melting temperature [3]. First wall materials in a fusion reactor will be subjected to radiation from X-rays and

neutrons, and significant ion fluxes with different types, energies, and intensities. The energy of ion fluxes is normally from several eV to 10's of MeV range [4]. In a D-T fusion reactor, neutrons and energetic ions such as tritium (T) and deuterium (D) particles impinge on tungsten, which induces a huge number of irradiation defects. This will thus influence the first wall properties and performance such as thermal conductivity and mechanical properties [5].

Low energy ions may cause significant surface erosion due to sputtering. It is important to gain knowledge of the microstructure evolution under irradiation of various energetic particles in order to predict the in-service behavior of tungsten components in a fusion reactor. The degree of irradiation damage of a target material including surface sputtering is dependent not only on the in-service irradiation environment but also the material characteristics such as crystal structure, surface roughness and so on. There are a huge database and well-established general models for the dependence of sputter yield on ion energy and incident ion angle. Although there have been also many reports on irradiation damage of tungsten in the literature [6–9], the effect of crystal orientation on the behavior of tungsten surface under energetic particle bombardment has not been fully investigated.

Optical diagnostics are an essential part of diagnostic systems of current and future fusion devices. In ITER and DEMO, all optical measurements have to be based on reflective optics [10, 11]. The most crucial of these systems will be the first mirrors (FMs) which are plasma-facing components of diagnostic schemes [10]. The main criterion to the FMs materials is high reflecting ability together with resistance to radiation damages due to the impact of 14 MeV neutrons from the D-T fusion reaction and charge exchange atoms (CXAs) – analog sputtering. Simultaneous impact of the neutrons and CXA can promote faster degradation of optical properties of the mirror in comparison with the impact of CXA only. Defects created by the neutrons in the near-surface layer can be a reason of faster change of surface morphology, and correspondingly, faster similar comparative experiments with tungsten, which was chosen to be one of the plasma-facing materials of in-vessel components of the ITER construction [9].

The effect of heavy sputtering and of neutron irradiation simulated by displacement damaging with of 20 MeV W^{6+} ions on the optical properties of tungsten mirrors has been previously studied [9]. Ar^{+} ions with 600 eV of energy were used as an imitation of charge exchange atoms ejected from fusion plasma. The ion fluence dependence of the surface topography and the optical properties of polycrystalline, recrystallized textured tungsten (grain size 20…100 μm) were studied by optical microscopy, interferometry, reflectometry, and ellipsometry. Furthermore, after sputtering in total a layer of 3.9 μm in thickness, the orientation and the thickness of the eroded layer of many individual grains was determined by electron backscattering diffraction and confocal laser scanning microscopy. The results of ellipsometry are rather intriguing since a quite large difference was found between parameters for specimens irradiated (3 dpa) and unirradiated with 20 MeV W^{6+} ions. A comparative analysis of experimental data obtained by reflectometry and ellipsometry made it possible to suggest a model of the process of surface modification for ITER-grade tungsten samples that were preliminarily irradiated with high energy tungsten ions. Two different scales in the surface roughness exist, namely, coarse-scaled and fine-scaled. The factor that is responsible for coarse-scaled roughness is sputtering, which is equal for both irradiated and unirradiated sides. As follows from results of [10], the neutron irradiation is connected with the defects created by neutrons in the near-surface layer. So, at the damage rate that would be achieved in ITER, it has already to make some additional contribution in the processes developing under the impact of charge exchange atoms only.

It is known now, that it is possible to obtain certain properties for W by controlling texture evolution. A texture is the sum of the different grain orientation. Typical techniques for forming the desired texture in metal usually refer to plastic deformation and combinations the annealing process between the mechanical deformation steps [12]. The thermo-mechanical processes will cause the lattices to reorient themselves along preferred directions by slip or twinning [13]. Unidirectional rolling will be a simple method to achieve texture transformation for tungsten. For W materials, most texture analyses have been conducted by Electron Backscattered Diffraction (EBSD) technique other than X-ray diffraction (XRD), like in Refs. [14, 15].

A.I. Belyaeva et al. [9, 16, 17] investigated the effect of sputtering on self-damaged recrystallized tungsten mirror specimens. The tungsten plate with the purity of 99.99 wt.% and with 99.7% of theoretical density was prepared (A.L.M.T. Corp., Japan) by powder metallurgy and hot-rolled reduction [18].

ITER-grade tungsten (W-IG), modified to fit the requirements of the reactor construction [9], was the initial material. A polycrystalline tungsten rod was subjected to forging in the radial direction [16] and then was annealed for 1 hour at 1000 ºC to remove the mechanical stress occurred during deformation. As a result, the grains are elongated perpendicular to the deformation direction and their crystallographic orientation correlates with it. Grains size is ~ 1…3 μm in width and up to 5 μm in length. W-IG manufacturing technology allows achieving high thermal conductivity normally to the surface. W-IG with grains elongated perpendicular to the surface has higher thermal conductivity and 2…10 times higher hydrogen retention than the material with the grains in the plane of the surface [18]. Tungsten is a bcc metal. Under radial compression, such metals acquire two preferential orientations: [100] and [110] [19]. As a result, deformation texture appears that is determined by manufacturing technology of ITER-grade tungsten. This is because a well annealed textured polycrystalline surface is typically composed primarily of the lowest surface-energy plane. It is important that in this case the technology (texture) ensures sputtering of all the indicated planes at the same angle.

The tungsten studied in [9, 16, 17] (W-rc) was obtained by W-IG tungsten recrystallization. The plate

was cut into specimens of 10×10×2 mm, double-sided mechanically and electrochemically polished to a high optical quality, and recrystallized at 2073 K for 1 h. The typical grain size was in the range 20…100 μm The recrystallized tungsten specimen was irradiated to 3 dpa by W^{6+} ions and sputtered by Ar^+ ions at a fluence of $6.45 \cdot 10^{23}$ m^{-2}. All grains with (111) or close orientations exhibited low sputtering yields, (110) displayed a higher yield and (100) grains showed a yield in the middle. The authors [9, 10, 16, 17] showed experimentally that for polycrystalline tungsten (bcc metal), the order of the three low-index surface energies is $\gamma_{(111)} > \gamma_{(100)} > \gamma_{(110)}$ (Fig. 1).

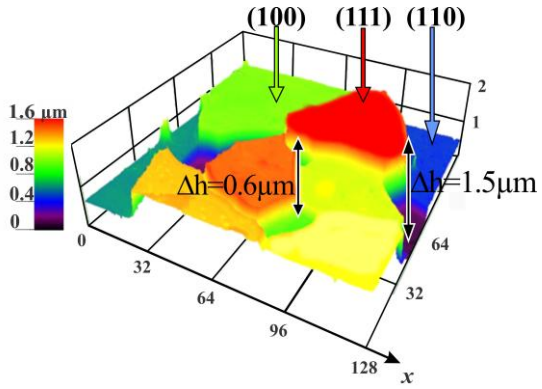

Fig. 1. EBSD results after the last sputtering (10^{23} m^{-2}) for 10×10 μm fragment of W-IG surface: orientation of some grains is specified (EBSD data). Height difference Δh between adjacent grains is indicated (inset – height scale) [16]

Stark et al. [20] have investigated the dependence of the sputter yield on the crystalline orientation with focused Ga^+ ion beam (FIB) bombardment of (001) single crystal W. A distinctive variation in the sputter yield with minima and maxima was observed in their study when the incident angle was changed. The positions of the minima of the observed sputter yield in the above study coincide with low-Miller-index crystalline orientations and were thus attributed to channeling of the Ga^+ ions. However, because their experiment was performed on a single crystalline sample with the changing incident angle, the effects of both crystal orientation and the incident angle were mixed together, thus cannot be individually distinguished in their results. For example, since the (001) orientation was bombarded with the normal incident angle that alone would lead to the least sputter yield while the other orientations were bombarded with higher incident angles, one cannot conclude that the orientation is more sputter resistant based on the lowest yield reported in their study.

On the other hand, the pure effect of crystal orientation has been revealed for commercially available polycrystalline tungsten was used where grains with different orientations were bombarded with the same normal incident angle. The effect of crystal orientation on the behavior of a tungsten surface under a 30 keV focused Ga^+ ion beam with different bombardment angles has been investigated by in situ scanning electron microscopy and electron backscatter diffraction [21]. Results indicate that the grains of tungsten with various orientations behave quite differently. Grains with a (001) direction parallel to the ion beam always maintain a much smoother surface morphology with less mass removal after ion bombardment, indicating a lower sputtering yield. The authors attributed the observed low surface erosion of (001) orientation to the relatively high binding energy of surface atoms and the large channeling effect of this low index orientation.

A clear relation between the tungsten grain orientation and both erosion and blister formation was fixed by authors [8, 22].

The surface topography and optical properties of polycrystalline recrystallized tungsten exposed to a low-energy (38 eV/D) high flux (10^{22} $m^{-2} \cdot s^{-1}$) deuterium plasma with an ion fluence of 10^{26} m^{-2} at various temperatures were investigated by authors [8]. Tungsten samples provided by A.L.M.T. Corp., Japan were mechanically polished to obtain a mirror-like surface and then recrystallized in vacuum at 1800 °C for 1 h. It was found that the surface morphology weakly depends on the exposure temperature in the range 320…695 K with the exception of the narrow temperature region around 535 K, where large changes to all optical characteristics occur. After plasma exposure at this temperature, the surface topography of the W sample is characterized by active blistering. It was found that the density of blisters is very inhomogeneous: e.g., in Fig. 2 two areas (~ 30×30 μm) with high (A) and low (B) blister density are emphasized.

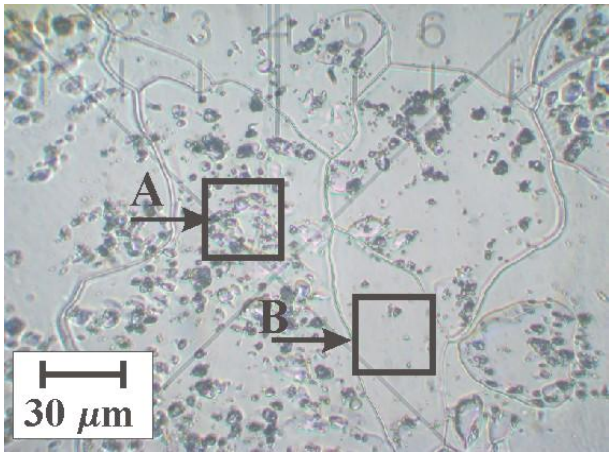

Fig. 2. Optical microscope image of recrystallized W sample exposed to a low-energy, high flux D plasma with an ion fluence of 10^{26} m^{-2} at T=535 K. Areas with high (A) and low (B) area density of blisters [8]

Later, it was shown that the presence of blisters was strongly correlated with the tungsten grain orientation. Strongest blistering is reported for grains with orientation close to (111) [22]. The presence of N in the plasma causes also blisters with cone-like shapes. He addition leads to the formation of flatter blisters and a very fine nano-porosity on the surface. W samples were exposed in the linear plasma generator PSI-2 at a sample temperature of 500 K with an incident ion flux of about 10^{22} $m^{-2} \cdot s^{-1}$, an incident ion fluence of $5 \cdot 10^{25}$ m^{-2} and an incident ion energy of 70 eV. Samples were exposed to pure D^+ plasma and with additional impurities of He (3%), Ar (7%), Ne (10%) or N (5%).

Blistering with grain orientation dependence was observed on all exposed samples. Most pronounced blistering was reported for grains with orientation close to (111). Highest erosion yield is observed for grains with orientation close to (100). The sample exposed to pure D^+ plasma reveals the presence of two groups of blisters with a size of few μm and about 200 nm. The addition of Ar or Ne results in surface erosion with different yields depending on grain orientation. Large blisters were present but show signatures of erosion. Less pronounced erosion is visible when adding N. The highest uptake of tritium was reported for the sample exposed to D+He plasma which corresponds to the largest – 18 nm, near-surface damage zone revealed by TEM. Lowest tritium accumulation was observed for samples exposed to D+Ar and D+Ne plasmas, which corresponds to the shallowest near-surface damage zone, as confirmed by TEM. It was shown that the presence of larger blisters and the erosion is strongly correlated with the tungsten grain orientation.

To better understand the grain orientation effect on erosion, EBSD analysis of the sample exposed to D-Ar mixed plasma was performed [22]. The blistering behavior should be attributed to the crystallographic orientation. For bcc metals, like tungsten, the preferred slip direction for plastic deformation is [111], which is perpendicular to the surface of grains oriented close to (111). In tungsten, grains oriented close to (001) all four [111] directions are at a shallow angle to the surface, which makes it less favorable for blistering to occur. The highest local erosion is observed for grains with orientation close to (001). The lowest erosion yield is observed for grains with orientation close to (101). This finding was in contradiction to results reported by other groups [8] where most pronounce erosion was found to occur for grains oriented close to (101) and lowest erosion yield for grains with orientation close to (111) (see Fig. 1). One has to notice, however, different irradiation conditions, namely, the energy of the impacting ions. In prior work [8] Ar ions with the energy of 600 eV were used. If the different sputtering behavior is true, it should be assigned to a different energy of sputtering Ar ions – in this case, the effect of grain orientation on sputtering would be energy-dependent. More work is required to confirm that observation.

Thus, it is very important to control the grain orientation of tungsten exposed to the bombardment of various ions. However, as it follows from the analysis of experimental data on tungsten sputtering carried out in this section, it is also important to take into account the sample manufacturing technology, power, and composition of the seeding gases, sputtering angle.

2. THEORETICAL METHOD ANALYSIS OF SURFACE ENERGY OF BCC TUNGSTEN

In the past few years, the methods for empirical and semi-empirical calculation surface energy of bcc metals have evolved rapidly. All of these methods are mathematically similar and have in common the attribute that the interaction between two atoms depends upon their local environment. It is mainly this fact that accounts for the huge successes that these methods have had in predicting effects at metallic surfaces where the atomic environment differs significantly from the bulk.

At present, the theory of the surface energy of metals does not make it possible to calculate this quantity with a sufficient accuracy. Estimation of configurational surface energy can be made using relationships of surface energy with such physical characteristics of crystals as sublimation heat, electron work function etc. The relationship between surface energy and sublimation heat is established using the following considerations. Sublimation heat characterizes the strength of bonds between atoms of a metal. Then the surface energy corresponds to the energy necessary to transfer an atom from the volume to the surface of the crystal, i.e., it is the energy of the broken bonds of an atom on the surface. Within this model equation (1) [23] allows us to calculate with a sufficient accuracy surface energy of metals at any temperature for different crystallographic planes with Miller indices (*hkl*):

$$\gamma_{(hkl)} = \frac{Z_S Z_{(hkl)}}{2Zf_{(hkl)}N_A}\left(\frac{\rho}{\mu A}\right)^{\frac{2}{3}}\left(E - 6RT\cdot\ln 2\right), \qquad (1)$$

where Z и Z_S are bulk and surface coordination numbers, respectively; $Z_{(hkl)} = Z - Z_S$ is the number of the breaking of bonds of atoms of surface; $f_{(hkl)}$ is nodal plane (*hkl*) packing factor; N_A is the Avogadro number; ρ is the density; A is the atomic mass; $\mu = 2$ is the basis of crystal cell; R is the universal gas constant; E is the sublimation energy.

In equation (1) one can see that the surface energy is directly proportional to the number of the breaking of bonds of atoms of the surface on the unit area:

$$\gamma_{(hkl)} \propto Z_{(hkl)}. \qquad (2)$$

A brief summary of the results, connected with the theoretical analysis of the surface energy anisotropy for the low-index crystal surfaces of the polycrystalline bcc tungsten is included in Table. For comparison, we present the first-principles calculation (FPC) and results of various theoretical methods. Surface energy can be calculated using the first-principles method within the framework of density-functional theory (DFT) [31, 32].

These theoretical methods (see Table) include FPC [26–32], the equivalent crystal theory method (ECT) [2], the tight-binding (TB) method [33], the jellium model [34], the embedded atom method (EAM) [35], the modified embedded atom method (MEAM) [36], the modified analytical embedded atom method (MAEAM) [37].

For all the theoretical models we know (their results are presented in Table), the high density (110) surface has the lowest energy for bcc metals. From Table, it is clearly seen that the calculated surface energy shows a strong anisotropy, the surface energy values of (100), (110) and (111) planes are different. Particularly puzzling is the fact that the FPC results [26–32] for W conform to the expected order of $\gamma_{(110)} < \gamma_{(100)}$. It is important to note that all of the AECT surface energy results from this study consistently support the trend $\gamma_{(110)} < \gamma_{(111)} < \gamma_{(100)}$ for bcc metals.

Tungsten (bcc metal) theoretical surface energies (hkl) ($J \cdot m^{-2}$)

Plane (*hkl*)	FPC [26–32]	AECT [2]	TB [33]	EAM [35]	MEAM [36]	MAEAM [37]	Wang et al. [24]	Zhang et al. [25]
(100)	4.635 [26], 5.100 [29], 4.780 [30]	5.904	6.700	2.809	2.646	2.882	4.025	2.645
(110)	4.005 [26], 3.840 [27]	3.279	4.300	2.599	2.232	2.638	2.998	2.232
(111)	4.452 [26]	4.319	6.750	–	2.247	3.315	3.671	2.247

This is also the trend obtained by MEAM [36] and authors [24, 25]. However, the results of the other theoretical model in Table do not always support this trend. In fact, the jellium model [34] and MAEAM model [34, 37] has $\gamma_{(111)} > \gamma_{(100)}$, that is confirmed experimentally (see Fig. 1). From Table, it can be seen that AECT surface energy results are closer FPC. However, it must be pointed out that experimental measurements of the surface energy are found for polycrystalline textured tungsten. Fu et al. [34] have used density functional theory to calculate the (100) surface energy in the bcc W. Their calculated value for W (5.1 $J \cdot m^{-2}$) is in good agreement with the value calculated using AECT and FPC.

The equivalent crystal nearest neighbor distance is a very vital parameter since it is needed for the calculation of surface energy.

3. DISCUSSION AND CONCLUSIONS

The following outline summarizes the main contributions of this manuscript.

Summarizing of the experimental and theoretical trends observed on the changes in surface microstructure and topography resulting from surface energy anisotropy for the low-index crystal surfaces of the polycrystalline bcc tungsten under sputtering is done. A brief summary of the most closely related work is included. The experimental results have been discussed in the framework of the various theoretical methods. Emphasis was placed on the problems which are existing up to now. It is shown that it is very important to control the grain orientation of tungsten exposed to the bombardment of various ions. However, from the analysis of experimental data on tungsten sputtering carried out in the study it follows, that it is also important to take into account the sample manufacturing technology, power and composition of the seeding gases along with the angle of sputtering. It is shown that the absence of a common trend in the ordering of the (100), (110), and (111) surface energies amongst the various theoretical models is a problem yet to be satisfactorily discussed.

We have in this study employed the set of analytical theoretical methods to provide a set of surface energy for bcc W. In this work, the (100), (110), and (111) surfaces were considered for the bcc tungsten. The surface energies of the bcc tungsten were found to be in good agreement with the available TB and MAEAM (see Table) calculations and experimental data (see Fig. 1). It has been found that the surface energy results from this study consistently support the trend, $\gamma_{(110)} < \gamma_{(100)} < \gamma_{(111)}$ for bcc W, which then shows that the densest packed bcc (110) surface posses the lowest energy. The other methods (see Table) support the trend, $\gamma_{(110)} < \gamma_{(111)} < \gamma_{(100)}$ for bcc W. Thus, the theoretical problem of calculating the surface energies of metals is still to be satisfactorily solved. The differences in the results obtained by the several theoretical methods are not yet small enough for us to begin to think that the different calculations have converged. This fact was unable to attribute the reason for these differences to the relaxation effects which were ignored since contributions from relaxation effects are usually small. Therefore the neglect of relaxation is excused.

The absence of a common trend in the ordering of the (100), (110), and (111) surface energies amongst the various theoretical models (see Table) is a problem yet to be satisfactorily discussed. In this work is not likely to have much effect on the accuracy of the calculated surface energies. We hope that the extensive results reported in this paper will be of help to those interested in the surface properties of metals. This research model can be further extended to the surface energy estimation of more crystals and surfaces. Clearly, more work should be done in this area. The orientation dependence of surface sputtering of tungsten can be used to guide the fabrication of tungsten-based first wall component and FMs in a nuclear fusion reactor.

Thus, it is very important to control the grain orientation of tungsten exposed to the bombardment of various ions. The experimental results of this manuscript (see Fig. 1), which include the non-roughening behavior and the least mass loss in the tungsten grains with (111) crystal orientation, cannot be explained by the existing theoretical models. Theoretical work on the effect of crystal orientation on the behavior of a target surface during ion beam bombardment is ongoing and will be reported in a future article.

REFERENCES

1. E. Lassner, W.D. Schubert. *Tungsten: Properties, Chemistry, Technology of the Element, Alloys and Chemical Compounds.* New York: Kluwer Academic/Plenum Publishers, 1999, 422 p.

2. E. Aghemenloh, J.O. Umukoro, S.O. Azi, S. Yusuf, J.O.A. Idiodi. Surface energy calculation of bcc metals using the analytical equivalent crystal theory method // *Comp. Mater. Sci.* 2011, v. 50, N 12, p. 3290-3296.

3. R.F. Radel, G.L. Kulcinski. Implantation of He^+ in candidate fusion first wall materials // *J. Nucl. Mater.* 2007, v. 367-370, p. 434-439.

4. G. Ran, X. Liu, J.H. Wu, N. Li, X.T. Zu, L.M. Wang. In situ observation of surface morphology evolution in tungsten under focused Ga^+ ion irradiation // *J. Nucl. Mater.* 2012, v. 424, N 1-3, p. 146-152.

5. Y. Watanabe, H. Iwakiri, N. Yoshida, K. Morishita, A. Kohyama. Formation of interstitial loops in tungsten under helium ion irradiation: Rate theory modeling and experiment // *Nucl. Instrum. Meth. B.* 2007, v. 255, p. 32-36.

6. A.F. Bardamid, A.I. Belyaeva, J.W. Davis, M.V. Dobrotvorskaya, A.A. Galuza, L.M. Kapitonchuk, V.G. Konovalov, I.V. Ryzhkov, A.F. Shtan', K.A. Slatin, S.I. Solodovchenko, V.S. Voitsenya. Optical properties of Al mirrors under impact of deuterium plasma ions in experiments simulating ITER conditions // *J. Nucl. Mater.* 2009, v. 393, N 3, p. 473-480.

7. N. Enomoto, S. Muto, T. Tanabe, J.W. Davis, A.A. Haasz. Grazing-incidence electron microscopy of surface blisters in single- and polycrystalline tungsten formed by H^+, D^+ and He^+ irradiation // *J. Nucl. Mater.* 2009, v. 385, N 3, p. 606-614.

8. A.I. Belyaeva, V.Kh. Alimov, A.A. Galuza, K. Isobe, V.G. Konovalov, I.V. Ryzhkov, A.A. Savchenko, K.A. Slatin, V.S. Voitsenya, T. Yamanishi. Optical characteristics of recrystallized tungsten mirrors exposed to low-energy, high flux D plasmas // *J. Nucl. Mater.* 2011, v. 413, N 1, p. 5-10.

9. A.I. Belyaeva, A.A. Savchenko, A.A. Galuza, I.V. Kolenov. Simultaneous impact of neutron irradiation and sputtering on the surface structure of self-damaged ITER-grade tungsten // *AIP Advances.* 2014, v. 4, N 7, p. 077121.

10. A.I. Belyaeva, A.A. Galuza, I.V. Kolenov, V.G. Konovalov, A.A. Savchenko, O.A. Skorik. Effect of Sputtering on the Samples of ITER-Grade Tungsten Preliminarily Irradiated by Tungsten Ions: Optical Investigations // *Phys. Met. Metallogr.* 2013, v. 114, N 8, p. 703-713.

11. V.S. Voitsenya, A.F. Bardamid, A.I. Belyaeva, V.N. Bondarenko, A.A. Galuza, V.G. Konovalov, I.V. Ryzhkov, A.A. Savchenko, A.N. Shapoval, A.F. Shtan', S.I. Solodovchenko, K.I. Yakimov. Modification of optical characteristics of metallic amorphous mirrors under ion bombardment // *Plasma Devices Oper.* 2009, v. 17, N 2, p. 144-154.

12. Pat. US 7101447 B2, USA. *Tantalum sputtering target with refine grains and uniform texture and method for manufacture* / S.P. Turner. Publ. 05.09.2006.

13. H. Hu. Texture of metals // *Texture.* 1974, v. 1, N 4, p. 233-258.

14. A.A. Galuza, A.D. Kudlenko, K.A. Slatin, A.I. Belyaeva, M.M. Smirnov. A system for the automation of a cryogenic spectral ellipsometer // *Instrum. Exp. Tech.* 2003, v. 46, N 4, p. 477-479.

15. A.F. Bardamid, A.I. Belyaeva, V.N. Bondarenko, A.A. Galuza, O.G. Kolesnyk, V.G. Konovalov, D.I. Naidenkova, I.V. Ryzhkov, A.N. Shapoval, C.H. Skinner, A.F. Shtan', S.I. Solodovchenko, V.S. Voitsenya, K.I. Yakimov. Behaviour of mirrors fabricated from amorphous alloy under impact of deuterium plasma ions // *Phys. Scripta.* 2006, v. T123, p. 89-93.

16. A.I. Belyaeva, O.A. Galuza, I.V. Kolenov, A.O. Savchenko. Role of recrystallization of tungsten in formation of a roughness of its surface under influence of successive action of neutrons and sputtering// *Metallofiz. Nov. Tekh.* 2016, v. 38, N 8, p. 1077-1102.

17. A.I. Belyaeva, A.A. Galuza, V.F. Klepikov, V.V. Litvinenko, A.G. Ponomarev, M.A. Sagajdachny, K.A. Slatin, V.V. Uvarov, V.T. Uvarov. Spectral ellipsometric complex for early diagnostics of metall and alloy transformations // *PAST.* 2009, N 2, p. 191-197.

18. W.M. Shu, G.-N. Luo, T. Yamanishi. Mechanisms of retention and blistering in near-surface region of tungsten exposed to high flux deuterium plasmas of tens of eV // *J. Nucl. Mater.* 2007, v. 367-370, p. 1463-1467.

19. T.H. Courtney. *Mechanical Behavior of Materials.* Long Grove: Waveland Press, 2005, 733 p.

20. Yu. Stark, R. Frömter, D. Stickler, H.P. Oepen. Sputter yields of single- and polycrystalline metals for application in focused ion beam technology // *J. Appl. Phys.* 2009, v. 105, N 1, p. 013542.

21. G. Ran, S. Wu, X. Liu, J. Wu, N. Li, X. Zu, L. Wang. The effect of crystal orientation on the behavior of a polycrystalline tungsten surface under focused Ga^+ ion bombardment // *Nucl. Instrum. Meth. B.* 2012, v. 289, p. 39-42.

22. M. Rasinski, A. Kreter, Y. Torikai, Ch. Linsmeier. The microstructure of tungsten exposed to D plasma with different impurities // *Nucl. Mater. Energy.* 2016 (in press).

23. C. Carter, M. Norton. *Ceramic Materials Science and Engineering.* New York: Springer Science+ Business Media, 2013, 766 p.

24. S.G. Wang, E.K. Tian, C.W. Lung. Surface energy of arbitrary crystal plane of bcc and fcc metals // *J. Phys. Chem. Solids.* 2000, v. 61, N 8, p. 1295-1300.

25. J.-M. Zhang, F. Ma, K.-W. Xu. Calculation of the surface energy of bcc metals by using the modified embedded-atom method // *Surf. Interface Anal.* 2003, v. 35, N 8, p. 662-666.

26. L. Vitos, A.V. Ruban, H.L. Skriver, J. Kollar. The surface energy of metals // *Surf. Sci.* 1998, v. 411, N 1-2, p. 186-202.

27. H.L. Skriver, N.M. Rosengaard. Surface energy and work function of elemental metals // *Phys. Rev. B.* 1992, v. 46, N 11, p. 7157-7168.

28. K. Kokko, P.T. Salo, R. Laihia, K. Mansikka. First-principles calculations for work function and surface energy of thin lithium films // *Surf. Sci.* 1996, v. 348 N 1-2, p. 168-174.

29. C.L. Fu, S. Ohnishi, H.J.F. Jansen, A.J. Freeman. All-electron local-density determination of the surface energy of transition metals: W(001) and V(001) // *Phys. Rev. B.* 1985, v. 31, N 2, p. 1168-1171.

30. J.C. Boettger. Nonconvergence of surface energies obtained from thin-film calculations // *Phys. Rev. B.* 1994, v. 49 N 23, p. 16798-16800.

31. G.-H. Lu, M. Huang, M. Cuma, F Liu. Relative stability of Si surfaces: A first-principles study // *Surf. Sci.* 2005, v. 588, N 1-3, p. 61-70.

32. D.-P. Ji, Q. Zhu, S.-Q. Wang. Detailed first-principles studies on surface energy and work function

of hexagonal metals // *Surf. Sci.* 2016, v. 651, p. 137-146.

33. M.J. Mehl, D.A. Papaconstantopoulos. Applications of a tight-binding total-energy method for transition and noble metals: Elastic constants, vacancies, and surfaces of monatomic metals // *Phys. Rev. B.* 1996, v. 54, N 7, p. 4519-4530.

34. J.P. Perdew, H.Q. Tran, E.D. Smith. Stabilized jellium: Structureless pseudopotential model for the cohesive and surface properties of metals // *Phys. Rev. B.* 1990, v. 42, N 18, p. 11627-11636.

35. A.M. Guellil, J.B. Adams. The application of the analytic embedded atom method to bcc metals and alloys // *J. Mater. Res.* 1992, v. 7, N 3, p. 639-652.

36. M.I. Baskes. Modified embedded-atom potentials for cubic materials and impurities // *Phys. Rev. B.* 1992, v. 46, N 5, p. 2727-2742.

37. Y.-N. Wen, J.-M. Zhang. Surface energy calculation of the bcc metals by using the MAEAM // *Comp. Mater. Sci.* 2008, v. 42, N 2, p. 281-285.

Article received 22.09.2017

АНИЗОТРОПИЯ ПОВЕРХНОСТНОЙ ЭНЕРГИИ НИЗКОИНДЕКСНЫХ КРИСТАЛЛИЧЕСКИХ ПОВЕРХНОСТЕЙ ТЕКСТУРИРОВАННОГО ПОЛИКРИСТАЛЛИЧЕСКОГО ОЦК-ВОЛЬФРАМА: ЭКСПЕРИМЕНТАЛЬНЫЙ И ТЕОРЕТИЧЕСКИЙ АНАЛИЗЫ

А.И. Беляева, А.А. Савченко, А.А. Галуза, И.В. Коленов

Проведены комплексный экспериментальный и теоретический анализы закономерностей в изменении микроструктуры и топографии низкоиндексных кристаллографических плоскостей поликристаллического ОЦК-вольфрама под влиянием распыления и связанных с анизотропией его поверхностной энергии. Приведен краткий обзор наиболее близких по теме работ. Экспериментальные результаты обсуждаются в рамках различных теоретических подходов. Акцент сделан на проблемах, нерешенных к настоящему времени. Показано, что различные современные теоретические подходы дают разные значения поверхностных энергий для плоскостей (100), (110) и (111) даже по порядку сравнения, и эта проблема на сегодняшний день не имеет удовлетворительного решения. Экспериментально показано, что для поликристаллического текстурированного вольфрама (ОЦК-металл) поверхностные энергии для трех низкоиндексных плоскостей имеют следующий порядок сравнения: $\gamma_{(111)} > \gamma_{(100)} > \gamma_{(110)}$.

АНІЗОТРОПІЯ ПОВЕРХНЕВОЇ ЕНЕРГІЇ НИЗЬКОІНДЕКСНИХ КРИСТАЛІЧНИХ ПОВЕРХОНЬ ТЕКСТУРОВАНОГО ПОЛІКРИСТАЛІЧНОГО ОЦК-ВОЛЬФРАМУ: ЕКСПЕРИМЕНТАЛЬНИЙ ТА ТЕОРЕТИЧНИЙ АНАЛІЗИ

А.І. Беляєва, А.О. Савченко, О.А. Галуза, І.В. Коленов

Проведено комплексний експериментальний та теоретичний аналізи закономірностей у зміненні мікроструктури і топографії низькоіндексних кристалографічних плоскостей полікристалічного ОЦК-вольфраму під впливом розпилення та пов’язаних з анізотропією його поверхневої енергії. Приведено короткий огляд найбільш близьких за тематикою робіт. Експериментальні результати обговорюються у рамках різноманітних теоретичних підходів. Акцент зроблено на проблемах, які не вирішені на цей час. Показано, що різноманітні сучасні теоретичні підходи дають різні значення поверхневої енергії для площин (100), (110) та (111) навіть за порядком порівняння, та ця проблема на цей час не має задовільного рішення. Експериментально показано, що для полікристалічного текстурованого вольфраму (ОЦК-метал) поверхневі енергії для трьох низькоіндексних площин мають такий порядок порівняння: $\gamma_{(111)} > \gamma_{(100)} > \gamma_{(110)}$.